Biomaterials 31 (2010) 2555–2564

Contents lists available at ScienceDirect

Biomaterials

journal homepage: www.elsevier.com/locate/biomaterials

# A hydrogel-based stem cell delivery system to treat retinal degenerative diseases

Brian G. Ballios [a], Michael J. Cooke [b], Derek van der Kooy [a,c], Molly S. Shoichet [a,b,d,*]

[a] Institute of Medical Science, University of Toronto, 1 King's College Circle, Toronto, Ontario M5S 1A8, Canada
[b] Department of Chemical Engineering and Applied Chemistry, University of Toronto, 200 College Street, Toronto, Ontario M5S 3E5, Canada
[c] Department of Molecular Genetics, University of Toronto, 1 Kings College Circle, Toronto, Ontario M5S 1A8, Canada
[d] Institute of Biomaterials and Biomedical Engineering, University of Toronto, 164 College Street, Room 407, Toronto, Ontario M5S 3G9, Canada

ARTICLE INFO

*Article history:*
Received 12 November 2009
Accepted 1 December 2009
Available online 6 January 2010

*Keywords:*
Hyaluronan
Hydrogel
Retina
Stem cell
Cell viability
Cell spreading

ABSTRACT

Regenerative strategies for retinal degenerative diseases are limited by poor cellular survival, distribution and integration after transplantation to the sub-retinal space. To overcome this limitations a stem cell delivery system was developed, taking advantage of the minimally-invasive, injectable and biodegradable properties of a blend of hyaluronan and methylcellulose (HAMC). The physical and biological properties of this unique HAMC formulation were studied. HAMC supported retinal stem-progenitor cell (RSPC) survival and proliferation *in vitro*. The blend was a viscous solution, exhibiting properties ideal for delivery to the sub-retinal space. *In vivo* transplantation studies in mice were carried out to investigate both the biodegradability of HAMC in the sub-retinal space over 7 days and the potential of HAMC as a cell delivery vehicle. RSPCs delivered in HAMC were more evenly distributed in the sub-retinal space than those delivered in traditional saline solutions, suggesting that HAMC is a promising vehicle for cellular delivery to the degenerating retina overcoming previously reported barriers to tissue integration in the retina such as cellular aggregation and non-contiguous distribution.



## 1. Introduction

Diseases of the retina and retinal function can lead to permanent loss of visual function for which there is no definitive treatment. The detrimental impact of vision loss on quality of life and activities of daily living has been well documented and affects the entire age spectrum. Retinitis pigmentosa (RP) affects the pediatric and young adult population, and is the leading cause of inherited retinal degeneration-associated blindness [1]. Diabetic retinopathy is the principle cause of blindness in middle-aged working adults [2]. Age-related macular degeneration (AMD) is the leading cause of irreversible blindness and moderate visual impairment in developed nations: there are an estimated 200,000 new cases annually in the United States [3]. Irreversible photoreceptor death or loss of function is common to all of these pathologies. It is expected that rates of blindness due to retinal degeneration will rise as our population ages in the coming decades [4,5], providing a strong impetus in the search for new therapies.

Current therapies for vision loss have focused predominantly on pharmacological treatments. For example, there have been recent advances in the treatment of the neovascular (wet) form of AMD with anti-vascular endothelial growth factor therapies [6,7]. Experimental treatments of diabetic retinopathy focus on bioactive molecules such as advanced glycosylation end product inhibitors and anti-oxidants to counter oxygen-induced injury [8]. While these therapies show promise in limiting the pathophysiologic advancement of the disease, they do not represent a restorative approach.

Cellular transplantation therapy is an alternate strategy, in which auto- or allogenic cellular material is used to replenish damaged retinal cells. The inner retinal microstructure in both AMD and RP is relatively intact following pathological photoreceptor degeneration, and one regenerative approach is to repopulate these cells without having to recapitulate the intricate retinal architecture. Various types of retinal tissue have now been allografted in the treatment of retinal disease: fetal retinal pigmented epithelium (RPE) cells to patients with AMD [9,10], and neural retinal cells to patients with RP [11]. Treating AMD by targeting RPE regeneration or transplantation is a therapeutically relevant option being pursued through research [12,13]. While graft survival is observed in some cases, improvements in visual acuity are disappointing to date [14].

Experimental research suggests that stem cell transplantation shows promise for reconstituting the damaged cellular populations of the retina [15,16]. One of the key advantages of using stem cells is

* Corresponding author. Donnelly Centre for Cellular and Biomolecular Research, 160 College St., Room 514, Toronto, Ontario M5S 3E1, Canada. Tel.: +1 416 978 1460; fax: +1 416 978 4317.
*E-mail address:* molly.shoichet@utoronto.ca (M.S. Shoichet).

0142-9612/$ – see front matter © 2009 Elsevier Ltd. All rights reserved.
doi:10.1016/j.biomaterials.2009.12.004

their potential to differentiate into any type of cell, including retinal neurons and RPE [17]. For cell replacement therapy in the retina, the discovery of adult retinal stem cells (RSCs) [18] and their isolation in humans [19] was a major step forward, avoiding the ethical concerns regarding the use of embryonic/fetal tissue [20]. It was shown that cells derived from the pigmented ciliary margin could give rise to all retinal cell types as well as integrate into the retinae of early postnatal mice [19]. The developing mouse eye is a permissive environment for cellular integration due to the presence of differentiation and proliferation signals and the absence of a mature glial limitans membrane, which prevents transplanted cells from migrating into the neural retina in adult intravitreal cellular transplantation [21]. To bypass this membrane in adults, the target for cellular replacement therapy is sub-retinal. Barriers to adult sub-retinal transplantation include cellular survival and host tissue integration. It has been well documented that cell death, leakage and migration from the injection site occurs when retinal progenitor cells are delivered as a single cell suspension in saline [22].

To overcome the poor survival and tissue integration associated with sub-retinal delivery, retinal progenitor cells have been delivered to the retina on solid biomaterial scaffolds [23–27]. These tissue engineered porous scaffolds are composed of common synthetic polymers including poly(L-lactic acid)/poly(lactic-co-glycolic acid) (PLLA/PLGA) [28], poly(methyl methacrylate) (PMMA) [26], poly(ε-caprolactone) (PCL) [24], or poly(glycerol-sebacate) (PGS) [23]. They are often coated with laminin to enhance cell adhesion and penetration into the porous polymer scaffold. While important advances have been made, these solid scaffolds do not match the modulus of the retina and lack the flexibility required for sub-retinal delivery across the damaged retina [27]. Injectable hydrogel-based materials, such as those investigated in this study, provide an alternative cell-delivery vehicle.

To overcome the barriers of cell survival and integration after sub-retinal transplantation, we propose to develop a minimally-invasive, injectable, and biodegradable vehicle for cellular delivery. Minimally-invasive ophthalmological procedures are associated with lower patient morbidity [29]. Using a minimally-invasive technique, the injection site would be self-healing without the need for sutures. Using a physical matrix, cells could be preloaded promoting even distribution after transplantation in the sub-retinal space. Importantly, by using a biodegradable biomaterial permanent retinal detachment due to material placement would not be a concern at the transplantation site. This would allow the tissue layers to heal together, and prevent pathologic fibrosis that disrupts normal retinal function.

To test our idea of an injectable hydrogel cell delivery vehicle to the sub-retinal space, we first screened a series of natural polymer hydrogels for physical properties of flow and gelation time, and biological properties of retinal stem-progenitor cell (RSPC) growth and cell survival. Agarose [30], collagen [31], chitosan/glycerol-phosphate [32], and HAMC (a physical blend of hyaluronan and methylcellulose) were included in the screen because all of these materials had literature precedence for injectability and simple gelation mechanisms. HAMC has been previously shown to exhibit rapid thermally-reversible gelation *in situ*, biocompatibility, biodegradability and a useful intrathecal drug delivery vehicle in the central nervous system (CNS) [33–35]. Based on these series of *in vitro* screens, HAMC was then pursued for *in vivo* studies where it was further evaluated for degradation and cell delivery. The HAMC formulation is particularly compelling because MC forms physical, hydrophobic crosslinks while HA is known to promote wound healing following CNS injection [33,36–38] and is non-immunogenic and biocompatible [39]. Moreover, HA is a prominent constituent of the interphotoreceptor matrix in humans, where it functions as a basic scaffold to which other macromolecules attach [40,41]. In this study, we developed a formulation and role for HAMC as a cell delivery vehicle by investigating cellular compatibility, *in vivo* biodegradability, and characteristics of integration of RSPCs in the sub-retinal space.

## 2. Materials and methods

### 2.1. Material preparation

Sodium hyaluronate (HA) was purchased from Novamatrix (1500 kDa; Drammen, Norway). HA was sterile-filtered as previously described [34]. Methylcellulose (MC, 300 kDa; Shin-Etsu, Tokyo) was sterilized in a similar manner, after dissolution in $ddH_2O$ on ice at 0.3 wt%. Sterile HAMC was prepared by dissolving HA and MC in aqueous media in a biological safety cabinet at the following mass ratios: 0.25/0.25, 0.50/0.50, 0.75/0.75, 1.00/1.00, 1.25/1.25 w/w%. The blends were mixed at 4 °C overnight. This aqueous media was either serum free media (SFM) [42] for cell culture *in vitro* or Hank's buffered saline solution (HBSS, Invitrogen, Burlington, ON) for transplantation *in vivo*.

Additional injectable hydrogels were prepared in saline for physical property evaluation, or cell culture media for *in vitro* experimentation. Type IX-Agarose (Sigma Aldrich, Oakville, ON) was prepared at 0.5% w/v; acid-soluble type I collagen (Nitta Gelatin Inc., Osaka, Japan) at 1% w/v; and a thermoreversible chitosan/glycerol-phosphate (GP) gel at 1% w/v [32].

### 2.2. Gelation time

In addition to physical flow through a 34G needle, the hydrogels were screened for gelation time as estimated using the inverted tube test [33].

### 2.3. In vitro characterization of cell survival and proliferation

All animal procedures were performed in accordance with the Guide to the Care and Use of Experimental Animals developed by the Canadian Council on Animal Care and approved by the Animal Care Committee at the University of Toronto. RSCs were derived from the ciliary epithelium of adult ACTB-GFP or -YFP mice as described previously [42]. Cells were plated in SFM on non-adherent tissue culture plates (Nunc; Thermo Fisher Scientific, Rochester, NY) at a density of 20 cells/μL. Floating spheres of cells grow from the clonal proliferation of single pigmented retinal stem cells to give rise to pigmented RPE progenitors and non-pigmented neural retinal progenitors, the second of which can differentiate into all retinal neuronal and glial subtypes [18,19].

Following 7 days of primary culture, spheres were either mixed directly with hydrogels reconstituted in growth media, or dissociated into a single cell suspension in a manner identical to pre-transplantation cell preparation (see below). Survival was assayed using fluorescence imaging and single cell counting, with ethidium homodimer-1 (EthD-1, 10 μM final concentration) (Invitrogen, Burlington, ON) used to mark dead cells. Proliferation was assayed by measuring the sphere diameter over 6 days of culture in the biomaterial matrix. Staining and fluorescence was visualized using a ZeissAxio Observer.D1 inverted fluorescent microscope equipped with an AxioCamMRm digital camera, and imaged using ZeissAxioVision V4.6 software. Significance is noted only if $p < 0.05$, as determined by using standard Student's *t*-test.

### 2.4. Fluorophore conjugation to HA and MC

HA and MC were modified with Alexa Fluor 488 hydrazide (Invitrogen, Burlington, ON) and Alexa Fluor 568 hydrazide, respectively, using carbodiimide chemistry as previously described by Kang et al. [34]. Fluorescently tagged HA and MC were sterile-filtered prior to use.

### 2.5. In vivo degradation profiles of fluorescently labeled HA and MC

The degradation profile of HA and MC was followed *in vivo* by measuring the fluorescence intensity over time. Fluorescently labeled HAMC was injected in the sub-retinal space (5 μL, 0.5/0.5 w/w %), as described in more detail in the transplantation protocol below. At $t = 0$, 6 h, 1, 3, 5, and 7 days after injection, animals were administered a lethal IP injection of sodium pentobarbital. To ensure the integrity of the neural retina and sub-retinal space, animals were perfused transcardially with saline and then 2% paraformaldehyde (PFA) immediately after sacrifice. Eyes were removed and placed in cold artificial cerebrospinal fluid (aCSF). Confocal image analysis using an Olympus Fluoview FV1000 microscope was performed on whole eyes with the cornea-lens-retinal axis perpendicular to the laser scanning direction to minimize refraction from the lens. This was used to obtain three dimensional reconstructions of the HA and MC in their native conformations post-injection in the sub-retinal space. The eyes were then dissected to remove autofluorescent extraocular muscle, as well as lens and vitreal attachments leaving only the posterior structures (neural retina and opposed RPE-choroid-sclera)

undisturbed. Subsequent epifluorescent and confocal imaging confirmed localization of HAMC to the sub-retinal space, and confocal image analysis software (Fluoview V2.0b) was used to quantify fluorescence intensity. Loss of fluorescence intensity per unit area was used as a measure of degradation for the HA and MC components. Values were corrected for background autofluorescence using non-injected tissue.

### 2.6. In vivo transplantation of RSPC loaded HAMC

Subretinal transplantation into the mouse eye was adapted from the technique described previously by Coles et al. [19]. $GFP^+$ RSPC spheres were dissociated into single cells with an enzymatic solution (trypsin 1.33 mg/mL, hyaluronidase 0.67 mg/mL, kynurenic acid 0.2 mg/mL,0.5 mg/mL collagenase I, 0.5 mg/mL collagenase II, 0.1 mg/mL elastase, Sigma Aldrich, Oakville, ON). The cells were resuspended in either HBSS or 0.5/0.5 w/w% HAMC to a concentration of 10,000 cells/μL. Animals were brought to a surgical plane of anesthesia with isoflurane. Using a 34 gauge beveled needle attached to the Nanofil submicrolitre injection system (World Precision Instruments, Sarasota, FL) 1 μL of cell suspension was injected into the sub-retinal space of adult CD10/Gnat2$^{-/-}$using a Möller Hi-R 900C surgical microscope (Innova Medical Ophthalmics, Inc., Toronto, ON). Four weeks after transplantation, animals were sacrificed and transcardially perfused with saline followed by 4% PFA. The eyes were removed and stored in 4% PFA (4 °C for 4 h), which was replaced with a 30% sucrose cryoprotectant solution (4 °C overnight). Tissue was placed in tissue fixative (FSC22 Frozen Section Compound; Richmond, IL) and frozen overnight at −80 °C. Frozen blocks were sectioned in a cryostat (−20 °C) at a thickness of 15 μm and mounted on Superfrost Plus Gold slides (Fisher Scientific, Ottawa, ON). Slides were then washed with Hoescht nuclear stain (Invitrogen, Burlington, ON) and reviewed by epifluorescence (ZeissAxio Observer.D1) to observe $GFP^+$ cells. The percentage of Bruch's membrane covered by $GFP^+$ transplanted cells integrated along the RPE was quantified using fluorescence intensity analysis in ImageJ.

## 3. Results

### 3.1. Biomaterial screening and selection

In order to determine the optimal biomaterial for cell delivery to the retina, we screened the following naturally-derived polymers that met our initial criteria of biodegradability, biocompatibility and injectability through a 34 gauge needle (85 μm inner diameter): HAMC, agarose, collagen, and chitosan/GP. These biomaterials were compared in terms of time to gelation and cellular response. A material that gelled between 10 and 60 min, using the simple inverted tube assay, was thought to be suitable in terms of handling *in vitro* and cell delivery *in vivo*, providing sufficient time for cell loading *in vitro* and cell distribution *in vivo* prior to gelation. Of the biomaterials tested, all met our time to gelation criterion except the chitosan/GP formulations (1% and 2%) and the weakest HAMC physical blend (0.25/0.25 w/w%, Fig. 1a). Of the HAMC physical polymer blends, the 0.5/0.5 and 0.75/0.75 w/w% passed the injectability screen. Higher weight percentages were not injectable through the 34 gauge needle, and were not considered further.

HAMC (0.5/0.5 and 0.75/0.75 w/w %), agarose and collagen were evaluated in terms of cellular response with cells cultured within each hydrogel and specifically in terms of RSPC growth *in vitro* relative to media controls. As RSPCs are normally cultured as spheres, sphere diameter was used as a proxy for cell growth with care taken to exclude the influence of sphere aggregation, as described further below. As shown in Fig. 1b and c, RSPC spheres increased in diameter in HAMC 0.5/0.5 similar to media controls. In HAMC 0.75/0.75, spheres increased in relative diameter similar to media controls, but did not reach the same absolute diameter after 6 days. Sphere mixing in HAMC 0.75/0.75, due to its higher viscosity, consistently resulted in reduced initial sphere diameter due to loss of cells from outer layers. Interestingly, sphere growth in collagen lagged significantly behind control growth media conditions in both absolute and relative diameter, and thus collagen was not pursued further. While the RSPC spheres grew to significantly higher diameters in agarose, the growth was characterized by cell spreading and morphological differentiation (Fig. 1f), suggesting loss of multipotency. Thus, agarose was removed from further consideration. In contrast, spheres plated in HAMC formulations exhibited similar relative growth as in media controls, but without cell spreading (Fig. 1b–e). Thus, further studies were pursued with HAMC 0.5/0.5 and 0.75/0.75.

It has been demonstrated that increases in primary RSPC sphere diameter can take place through two processes: proliferative cell division [43] and aggregation and merging of smaller spheres [44]. In order to separate these two phenomena and validate the sphere diameter assay as a measure of proliferation, individual spheres were counted (Fig. 1g). Approximately 5 spheres per well chosen from primary cultures were plated in HAMC and control media, and counted over 6 days. There was no change in the number of spheres per well, indicating that cells were proliferating rather than spheres coalescing. For the latter to have been true, the number of spheres would have decreased.

### 3.2. In vitro characterization of stem cells in HAMC

Prior to studying HAMC as a cell delivery vehicle *in vivo*, cell viability and cell distribution were studied *in vitro* over 6 days for both spheres and single cell suspensions. Live cells, identified as GFP-positive and EthD-negative, were constant across all culture conditions (media, HAMC 0.5/0.5 and HAMC 0.75/0.75) for spheres (Fig. 2a) and single cells (Fig. 2b). While there was no significant difference across the groups at each time point, there was a decrease in cell viability after 3 days of culture of single cells (in all conditions) relative to both time of plating ($t = 0$) and spheres. RSPC sphere diameter, reflective of proliferative cell division, was not significantly different between control media and the HAMC 0.5/0.5 blend over 6 days: day 0: media $84 \pm 2$ μm vs. HAMC $71 \pm 11$ μm; day 3: media $103 \pm 7$ μm vs. HAMC $83 \pm 15$ μm; day 6: media $130 \pm 17$ μm vs. HAMC $142 \pm 4$ μm.

To better understand the suitability of HAMC as a cell delivery vehicle, cell distribution was studied and imaged by confocal reconstruction of a single cell suspension of RSPCs at 37 °C after 6 days of culture. As shown in Fig. 2e, RSPCs were homogeneously (and stably) distributed within the HAMC matrix unlike the distribution in media where cell aggregation was evident (data not shown). This demonstrates that HAMC prevents cellular aggregation, which may be important for cell integration in the host tissue [22]. We did not observe an appreciable difference between HAMC 0.5/0.5 and HAMC 0.75/0.75 and thus chose to pursue only HAMC 0.5/0.5 in further analysis because this blend was easier to inject through the 34 gauge needle.

### 3.3. In vivo degradation profile of HAMC in the sub-retinal space

The *in vivo* degradation profile of HAMC (0.5/0.5) was followed by measuring the depletion in fluorescence intensity of fluorescently-tagged Alexa Fluor 488-HA and Alexa Fluor 568-MC over 7 days. The fluorescently-tagged HAMC blend was injected into the sub-retinal space of adult albino mice (see below) and visualized by confocal microscopy immediately after injection and then over time to determine the degradation profile (Fig. 3).

Fluorescence was quantified and normalized to day 0 controls using image analysis software. Both HA and MC exhibited rapid degradation within the first 6 h after transplantation. HA exhibited a more rapid degradation over time, dropping to approximately 10% of initial levels within 3 days and falling to a minimum of approximately 3% after one week. In contrast, MC showed persistence within the sub-retinal space to approximately 20% of its initial value after 7 days.

### 3.4. Transplantation of RSPCs in HAMC

To evaluate the utility of HAMC for cell delivery, primary culture RSPCs isolated from beta-actin-GFP transgenic mice

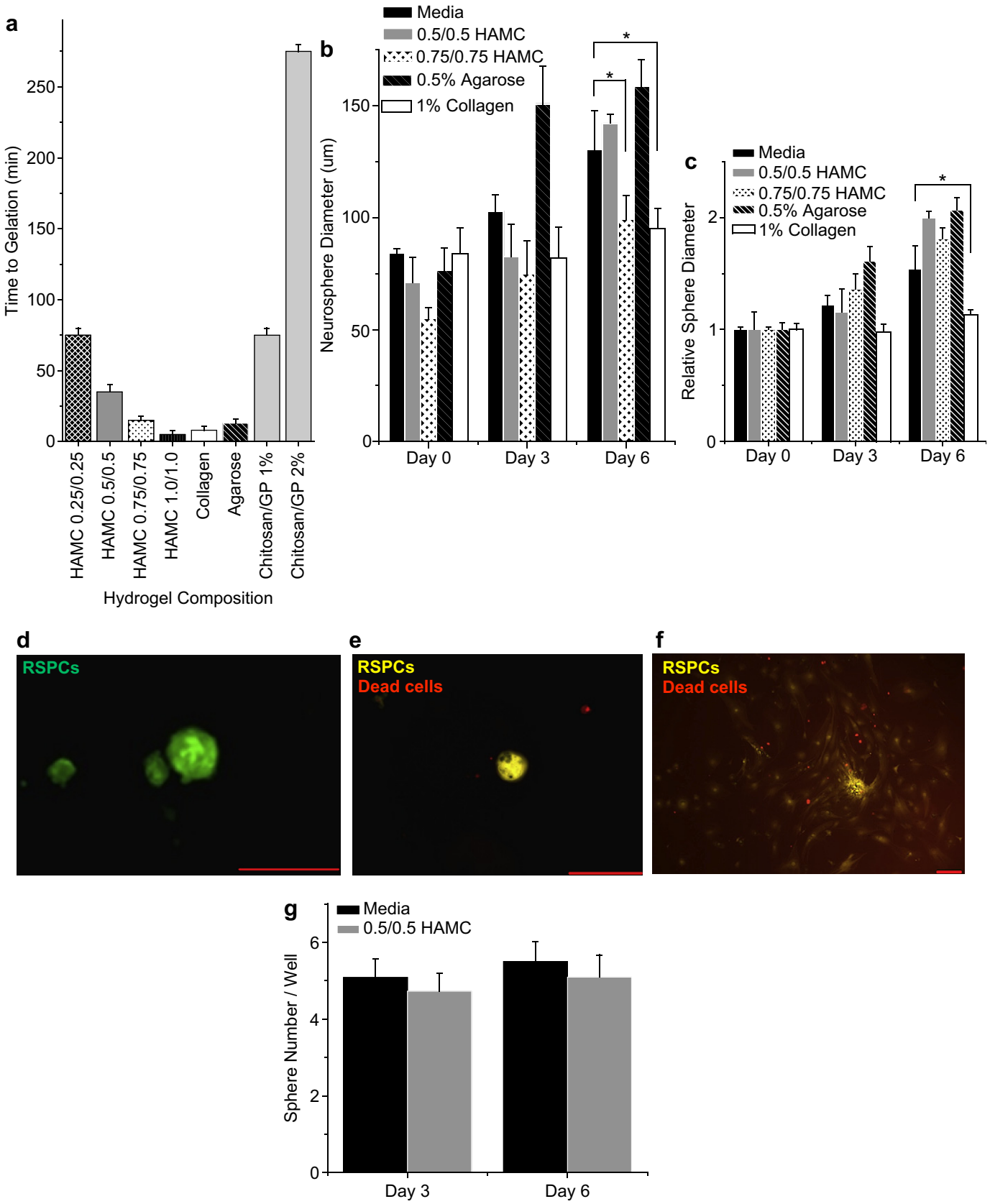


**Fig. 1.** Vehicle screening trials. Time to gelation by inverted tube test for (a) various screened cell delivery vehicles and various HAMC compositions. Sphere diameters *in vitro* as (b) absolute and (c) relative to day 0, assayed in control growth media, agarose, collagen, and HAMC. Representative images showing $GFP^+$ and $YFP^+$ RSPC spheres plated in (d) control growth media, (e) 0.5/0.5% HAMC, and (f) 0.5% w/v agarose illustrating cell spreading (red, EthD1 dead cell staining, scale 200 μm). (g) RSPC sphere counting comparing sphere growth in control growth media to 0.5/0.5% HAMC. Culture data pooled from cultures performed in triplicate ($n > 3$ per culture). Error bars represent SD (* $p<0.05$).

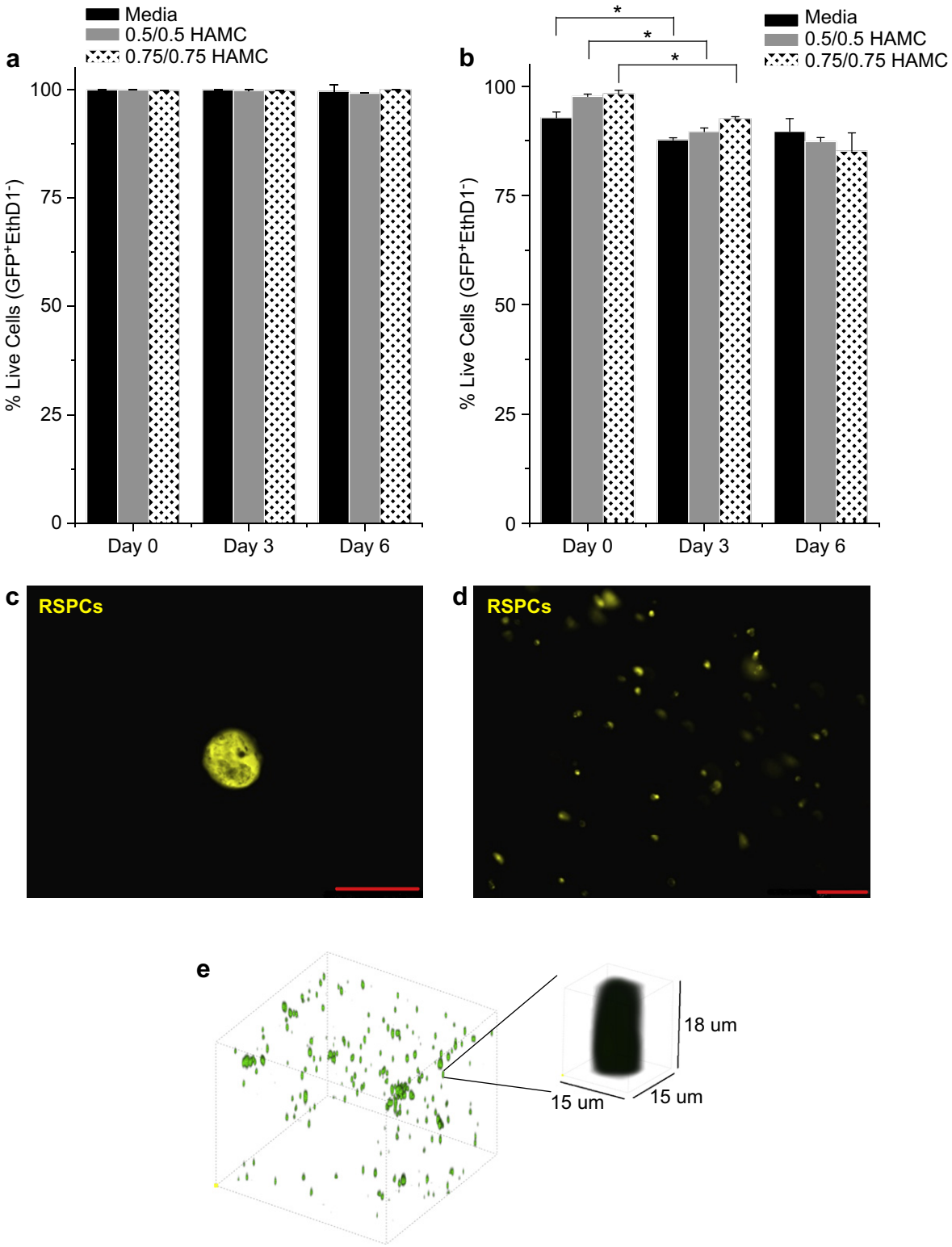


**Fig. 2.** *In vitro* characterization of RSPC loaded HAMC. Viability data for cells distributed in 0.5/0.5% HAMC as (a) whole spheres and (b) dissociated sphere single-cell suspension. Representative micrographs of (c) a whole sphere and (d) dissociated sphere suspensions in HAMC over 6 day culture (scale 100 μm). Note, some dissociated cells are out of the plane of focus. (e) Confocal reconstruction of dissociated $GFP^+$ RSPC suspension in 0.5/0.5% HAMC illustrating random cellular distribution and inhibition of cellular aggregation and settling (volume: 1.7 $mm^3$). Single cell included for scale. Culture data pooled from cultures performed in triplicate ($n > 3$ per culture). Error bars represent SD (* $p<0.05$).

were dissociated to single cells and injected into the sub-retinal space of adult CD10/Gnat2$^{-/-}$mice at a concentration of 10,000 cells/μL in either HAMC or saline alone. Mutation of the Gnat2 gene leads to cone dysfunction and progressive loss, which is a predictive and reliable measure of AMD severity [45].

Tissue analysis at 4 weeks following injection revealed that RSPCs delivered in saline alone resulted in non-continuous banding

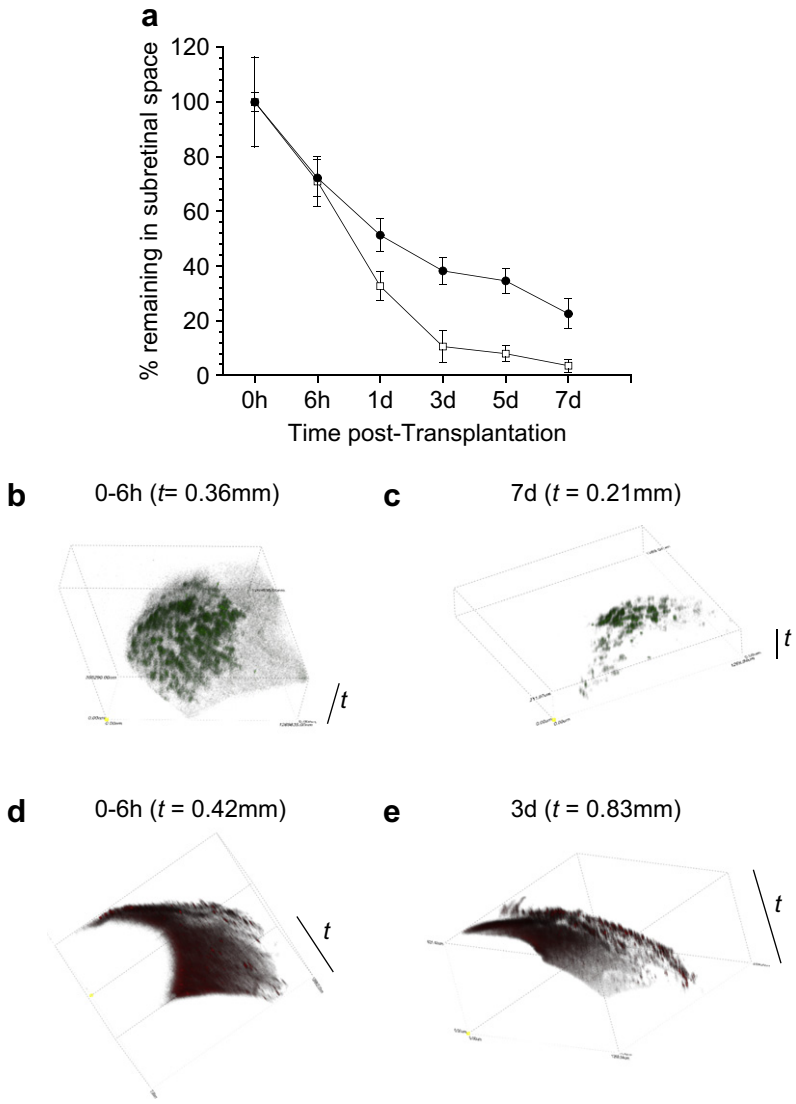


**Fig. 3.** *In vivo* characterization of HAMC degradation in the sub-retinal space. (a) Mass loss curves (% remaining) of HA (□)and MC (●)over 7 days as assessed by confocal microscopy of fluorescently-labeled components ($n = 4$ eyes analyzed per time point). Representative images from (b, c) HA and (d, e) MC degradation time courses. Confocal reconstructions are over an area of 1.3 × 1.3 mm of tissue, with tissue thickness ($t$) as indicated. Note the punctate appearance throughout the HA component within 6 h of injection compared to MC.

patterns in the RPE (Fig. 4a). In contrast, RSPCs delivered in HAMC (0.5/0.5) integrated with the RPE and formed continuous banding patterns (Fig. 4b). The cellular morphology of the GFP-positive and nuclear-stained transplanted cells was consistent with the cuboidal epithelium characteristic of RPE cells, sitting atop Bruch's membrane (BM) (Fig. 4c–f). In order to quantify this increase in cellular distribution seen with HAMC, the percentage of Bruch's membrane covered by $GFP^+$ cells was quantified using image analysis software. Delivery with HAMC resulted in a significant increase in coverage over buffered saline vehicle (Fig. 4g): 93% with HAMC vs. 50% with saline. Of note, between four and five GFP-positive cells per eye appeared in opposition to the outer nuclear layer (ONL) amidst photoreceptor outer segments (Fig. 4h–k), and this was not different between HAMC or saline vehicles. Qualitatively, there was no observed effect of HAMC versus saline injection on retinal morphology in terms of overall thickness, laminar integrity or the appearance of the ONL and RPE/Bruch's membrane. Taken together, delivering RSPCs in HAMC had a dramatic effect on cellular distribution within the host tissue, with a marked reduction in cellular aggregation and improved distribution over the RPE/Bruch's membrane.

## 4. Discussion

HAMC, of the biomaterials screened, was evaluated *in vivo* for cell delivery based on criteria of injectability, time to gelation and neutral effect on growth kinetics. This allowed us to eliminate a number of commonly studied materials while providing a rationale for the use of HAMC.

Importantly, HAMC impacted neither cell survival nor normal cellular growth. Cell survival and proliferation were assessed separately in this study, a distinction that has been neglected in previous biomaterial-cell delivery studies [23,46]. We demonstrated that sphere growth is a good proxy for proliferation and not sphere aggregation. These results are consistent with those of Mori et al. who showed that coalescence in neural stem cell culture is observed only from the merging of small cell aggregates in immature cultures but not by mature neurospheres [44]. We

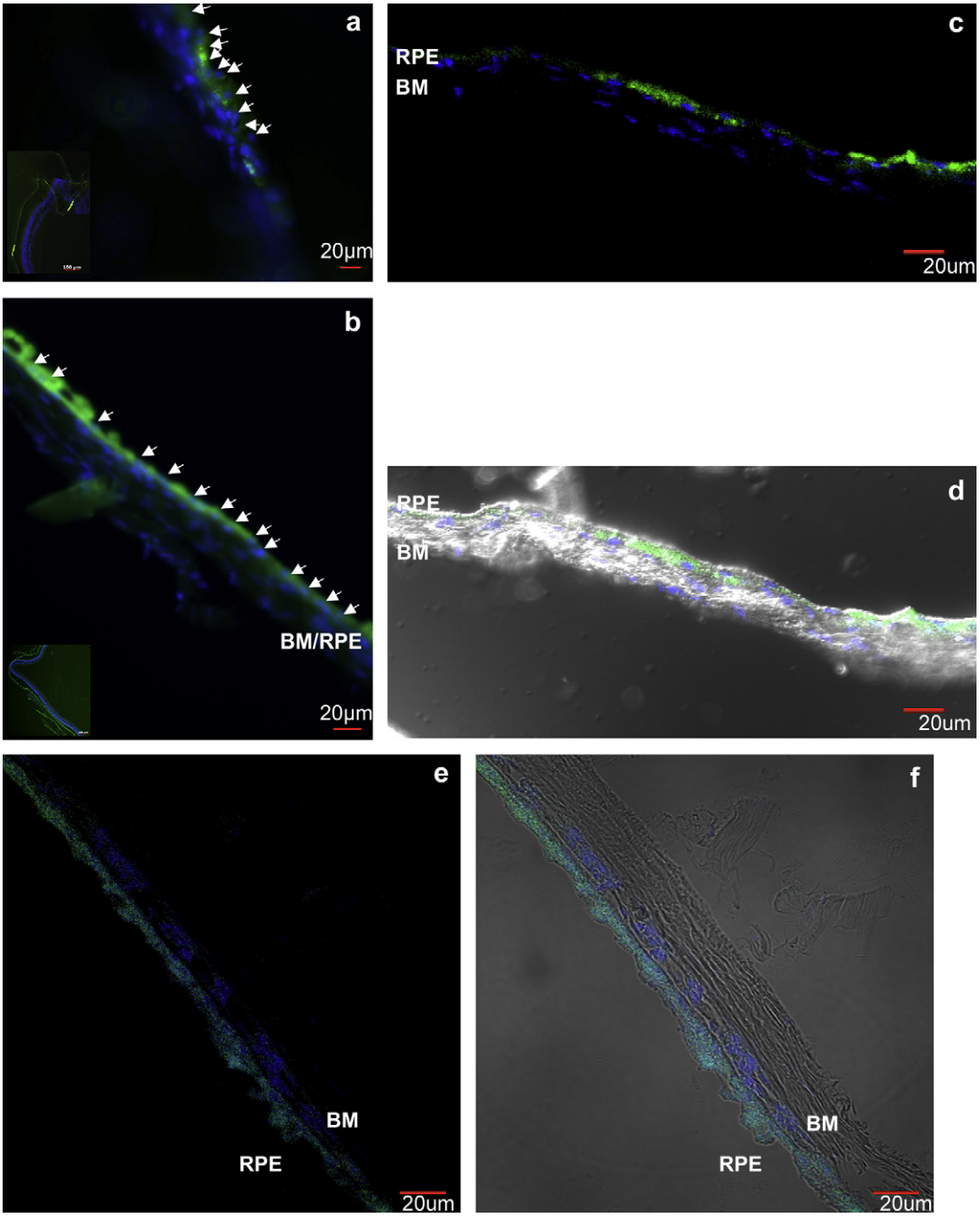


**Fig. 4.** *In vivo* adult sub-retinal transplantation of GFP$^+$RSPCs in HAMC, assayed at 4 weeks post-transplantation. (a) Control transplantation in saline vehicle show non-contiguous cellular integration and localized cellular groupings (inset) atop Bruch's membrane (BM), suggestive of cellular aggregation pre- or post-transplantation. (b) Transplantation in HAMC shows contiguous areas of RPE integration over large areas of retina (inset), suggesting HAMC maintains cellular distribution during injection and preventing aggregation pre- or post-transplantation. Arrowheads indicate location of nuclei of transplanted cells. Confocal images of cuboidal RPE cells sitting atop Bruch's membrane after injection in (c) saline and (e) HAMC (c,e, Hoechst and GFP; d,f, merge with DIC to show cytoplasm). Note non-contiguous distribution in buffered saline vehicle versus HAMC. (g) Integration along the RPE shows significantly greater coverage of Bruch's membrane by GFP$^+$ cells delivered in HAMC versus buffered saline over integrated areas ($n = 3$ eyes each). Cells located in opposition to the ONL intermingled within ONL cytoplasmic extensions (h and j show blue-Hoechst and GFP fluorescence; i and k show these images merged with the DIC-imaged cytoarchitecture). (i-ii) RSPC/saline injection and (iii-iv) RSPC/HAMC injection (* $p<0.05$).

observed more consistent cell viability over culture time of the spheres vs. single cells, yet chose to inject single cells because sphere diameter limits injectability through the 34 gauge needle in the sub-retinal transplant and ultimately single cells are likely to integrate with the host tissue better. While survival of single cells was high in both HAMC and control media over time, the drop in viability may reflect loss of autocrine/paracrine signaling between cells, such as endogenous secretion of FGF2 by closely associated cells, as is normally observed in RSPC sphere colonies [18,19].

Importantly, HAMC maintains a distribution of cells during the *in vitro* cell culture, as demonstrated by confocal reconstruction. Thus, HAMC overcomes the problems of cellular

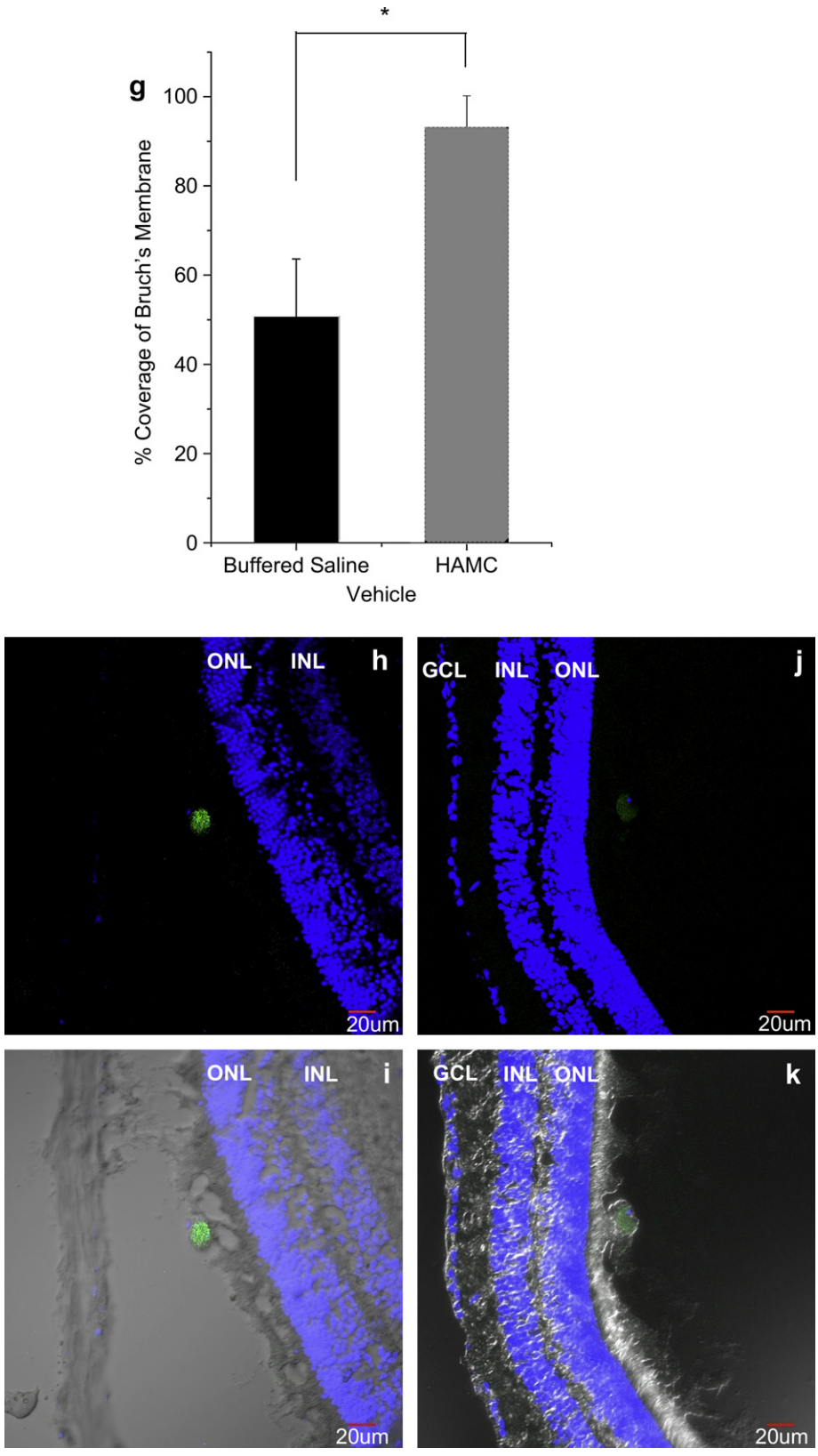


**Fig. 4** (*continued*).

aggregation and provides greater opportunity for cellular integration with host tissue. Cells dispersed in HAMC did not aggregate over the 6 day culture period, providing further evidence that mixing cells in HAMC inhibits cellular aggregation prior to transplantation. These cell distribution phenomena are not often studied in the context of cellular delivery using injectable biomaterials, but are essential to anticipating and understanding the behavior of the system *in vivo*.

The *in vivo* experiments confirm the potential of HAMC as a minimally-invasive, injectable and biodegradable cell delivery vehicle. The ability to inject a fluidic vehicle without the inherent risk of retinal microstructure damage that might arise during the placement of a solid, cell-seeded scaffold confers an important practical benefit. The use of this cell delivery vehicle is a step towards the development of safe biomaterials for the treatment of retinal diseases. HAMC is viscous on injection, with no observed backflow on needle retraction or clogging of the 34 gauge needle. Its non-cell adhesive properties [33] minimize scar formation and its biologically neutral impact on cell survival and growth allows transplanted cells to respond to endogenous cues that may promote integration.

Dissection and fluorescent labeling combined with confocal reconstruction indicated that HAMC filled the sub-retinal space evenly and degraded over a one week period. No changes in retinal morphology were observed. The *in vivo* degradation profile of both HA and MC in the sub-retinal space was slower than that observed in the intrathecal space [34], where similar materials have been used previously, likely because of continuous CSF flow in the intrathecal space which is absent in the sub-retinal space. However, similar to the intrathecal studies, HA was observed to degrade more rapidly than MC. Endogenous hyaluronidase is present in the normal eye [47] and pathologic retina [48], and can serve to degrade the HA. In support of these known mechanisms of HA degradation this component showed a punctate appearance within the first few hours following injection. This corresponds to bulk degradation throughout the entire material, contrasted with surface degradation which would show preferential erosion of HA fluorescence at the periphery. This is consistent with previous work, which shows that HAMC presents minimal resistance to molecular diffusion of molecules up to 150 kDa [35]. Therefore, hyaluronidase (53.9 kDa) may diffuse freely throughout the gel.

Compared to saline delivery of RSPCs, HAMC delivery decreased cellular aggregation and promoted cellular distribution in the sub-retinal space. Following transplantation, the majority of cells integrate in the RPE layer, adopting a cuboidal morphology. This cell delivery strategy may be useful for the treatment of widespread or advanced maculopathy, where large areas of the RPE are destroyed [45]. The choroidal neovascularization inherent in wet-AMD is marked by widespread disruption of the RPE and disturbance of the homeostatic mechanisms of photoreceptor outer segment phagocytosis [49–51]. The RPE replacement potential demonstrated by the HAMC delivery system is therefore therapeutically relevant to the treatment of AMD.

Efficient cell delivery and survival are major barriers to successful cellular transplantation in the CNS. Most transplanted cells die, and those that remain viable either migrate away from the transplant site and/or aggregate together and thus do not integrate with the host tissue [22]. The data presented here show that, through the use of innovative biomaterial engineering, cell delivery in HAMC promotes tissue integration without compromising cell survival. While there are a few other reports of biodegradable polymeric scaffolds studied for cell transplantation in the retina [23–27], this is the first report to test and demonstrate the benefit of an injectable biodegradable polymer as a vehicle for the delivery of cells versus a single-cell suspension in saline. The cellular integration observed is significantly better when cells are delivered in HAMC vs. saline alone. The use of HAMC as a minimally invasive, injectable and biodegradable strategy for cell delivery to the damaged retina demonstrates the benefit of an appropriately designed biomaterial for greater success of cell therapy in the CNS.

## 5. Conclusions

A hydrogel-based system for cellular delivery that allows localized delivery to the sub-retinal space was developed and characterized. A formulation of HAMC meets the design criteria of being minimally-invasive, injectable and biodegradable *in situ*. The vehicle allows RSPC survival and proliferation *in vitro*, and exhibits benefits in overcoming barriers to cell integration in the *in vivo* studies when compared to saline controls. This system will now be further investigated and adapted for the delivery of therapeutic cellular populations for the regeneration of vision in animal models of retinopathy.

## Conflicts of interest

The authors confirm that there are no known conflicts of interest associated with this publication and there has been no significant financial support for this work that could have influenced its outcome.

## Acknowledgements

The authors are grateful to the following individuals: Brenda Coles (for general technical and cell culture support), Laura Clarke (for assistance with transplantation) and Drs. Tasneem Zahir and Yakov Lapitsky (for assistance with development of the HAMC hydrogel). Funding for this study was provided by NSERC (MSS) and the NIH (DvdK). BGB is supported by the CIHR MD/PhD studentship, a McLaughlin Centre Graduate Fellowship, a University of Toronto Open Fellowship and the McLaughlin Centre for Molecular Medicine.

## Appendix

Figures with essential color discrimination. Figs. 1, 2, 3 and 4 in this article are difficult to interpret in black and white. The full color images can be found in the on-line version, at doi:10.1016/j.biomaterials.2009.12.004.

## References

[1] Shintani K, Shechtman DL, Gurwood AS. Review and update: current treatment trends for patients with retinitis pigmentosa. Optometry 2009;80:384–401.
[2] Klein BEK. Overview of epidemiologic studies of diabetic retinopathy. Ophthalmic Epidemiol 2007;14:179–83.
[3] Kaufman SR. Developments in age-related macular degeneration: diagnosis and treatment. Geriatrics 2009;64:16–9.
[4] Congdon NG, Friedman DS, Lietman T. Important causes of visual impairment in the world today. J Am Med Assoc 2003;290:2057–60.
[5] Lee P, Wang CC, Adamis AP. Ocular neovascularization: an epidemiologic review. Surv Ophthalmol 1998;43:245–69.
[6] Rosenfeld PJ, Brown DM, Heier JS, Boyer DS, Kaiser PK, Chung CY, et al. Ranibizumab for neovascular age-related macular degeneration. N Engl J Med 2006;355:1419–31.
[7] Menon G, Walters G. New paradigms in the treatment of wet AMD: the impact of anti-VEGF therapy. Eye 2009;23(Suppl. 1):S1–7.
[8] Comer GM, Ciulla TA. Current and future pharmacological intervention for diabetic retinopathy. Expert Opin Emerg Drugs 2005;10:441–55.
[9] Algvere PV, Gouras P, Kopp ED. Long-term outcome of RPE allografts in non-immunosuppressed patients with AMD. Eur J Ophthalmol 1999;9:217–30.
[10] Algvere PV, Berglin L, Gouras P, Sheng Y. Human fetal RPE transplants in age related macular degeneration (ARMD). Invest Ophthalmol Vis Sci 1996;37:S96.
[11] Das TP, Del Cerro M, Lazar ES, Jalali S, DiLoreto DA, Little CW, et al. Transplantation of neural retina in patients with retinitis pigmentosa. Invest Ophthalmol Vis Sci 1996;37:S96.
[12] Chen FK, Uppal GS, Maclaren RE, Coffey PJ, Rubin GS, Tufail A, et al. Long-term visual and microperimetry outcomes following autologous retinal pigment epithelium choroid graft for neovascular age-related macular degeneration. Clin Experiment Ophthalmol 2009;37:275–85.
[13] Da Cruz L, Chen FK, Ahmado A, Greenwood J, Coffey P. RPE transplantation and its role in retinal disease. Prog Retin Eye Res 2007;26:598–635.
[14] Berson EL, Jakobiec FA. Neural retinal cell transplantation: ideal versus reality. Ophthalmology 1999;106:445–6.
[15] Klassen H, Sakaguchi DS, Young MJ. Stem cells and retinal repair. Prog Retin Eye Res 2004;23:149–81.

[16] Enzmann V, Yolcu E, Kaplan HJ, Ildstad ST. Stem cells as tools in regenerative therapy for retinal degeneration. Arch Ophthalmol 2009;127:563–71.
[17] Das AM, Zhao X, Ahmad I. Stem cell therapy for retinal degeneration: retinal neurons from heterologous sources. Semin Ophthalmol 2005;20:3–10.
[18] Tropepe V, Coles BLK, Chiasson BJ, Horsford DJ, Elia AJ, McInnes RR, et al. Retinal stem cells in the adult mammalian eye. Science 2000;287:2032–6.
[19] Coles BLK, Angenieux B, Inoue T, Rio-Tsonis K, Spence JR, McInnes RR, et al. Facile isolation and the characterization of human retinal stem cells. Proc Natl Acad Sci USA 2004;101:15772–7.
[20] Sugarman J. Human stem cell ethics: beyond the embryo. Cell Stem Cell 2008;2:529–33.
[21] Kinouchi R, Takeda M, Yang L, Wilhelmsson U, Lundkvist A, Pekny M, et al. Robust neural integration from retinal transplants in mice deficient in GFAP and vimentin. Nat Neurosci 2003;6:863–8.
[22] Klassen HJ, Ng TF, Kurimoto Y, Kirov I, Shatos M, Coffey P, et al. Multipotent retinal progenitors express developmental markers, differentiate into retinal neurons, and preserve light-mediated behavior. Invest Ophthalmol Vis Sci 2004;45:4167–73.
[23] Redenti S, Neeley WL, Rompani S, Saigal S, Yang J, Klassen H, et al. Engineering retinal progenitor cell and scrollable poly(glycerol-sebacate) composites for expansion and subretinal transplantation. Biomaterials 2009;30:3405–14.
[24] Redenti S, Tao S, Yang J, Gu P, Klassen H, Saigal S, et al. Retinal tissue engineering using mouse retinal progenitor cells and a novel biodegradable, thin-film poly(e-caprolactone) nanowire scaffold. J Ocul Biol Dis Infor 2008;1:19–29.
[25] Neeley WL, Redenti S, Klassen H, Tao S, Desai T, Young MJ, et al. A microfabricated scaffold for retinal progenitor cell grafting. Biomaterials 2008;29:418–26.
[26] Tao S, Young C, Redenti S, Zhang Y, Klassen H, Desai T, et al. Survival, migration and differentiation of retinal progenitor cells transplanted on micro-machined poly(methyl methacrylate) scaffolds to the subretinal space. Lab Chip 2007;7:695–701.
[27] Tomita M, Lavik E, Klassen H, Zahir T, Langer R, Young MJ. Biodegradable polymer composite grafts promote the survival and differentiation of retinal progenitor cells. Stem Cells 2005;23:1579–88.
[28] Lavik EB, Klassen H, Warfvinge K, Langer R, Young MJ. Fabrication of degradable polymer scaffolds to direct the integration and differentiation of retinal progenitors. Biomaterials 2005;26:3187–96.
[29] Kubitz JC, Motsch J. Eye surgery in the elderly. Best Pract Res Clin Anaesthesiol 2003;17:245–57.
[30] Tschon M, Fini M, Giavaresi G, Torricelli P, Rimondini L, Ambrosio L, et al. In vitro and in vivo behaviour of biodegradable and injectable PLA/PGA copolymers related to different matrices. Int J Artif Organs 2007;30:352–62.
[31] Wallace DG, Rosenblatt J. Collagen gel systems for sustained delivery and tissue engineering. Adv Drug Deliv Rev 2003;55:1631–49.
[32] Chenite A, Chaput C, Wang D, Combes C, Buschmann MD, Hoemann CD, et al. Novel injectable neutral solutions of chitosan form biodegradable gels in situ. Biomaterials 2000;21:2155–61.
[33] Gupta D, Tator CH, Shoichet MS. Fast-gelling injectable blend of hyaluronan and methylcellulose for intrathecal, localized delivery to the injured spinal cord. Biomaterials 2006;27:2370–9.
[34] Kang CE, Poon PC, Tator CH, Shoichet MS. A new paradigm for local and sustained release of therapeutic molecules to the injured spinal cord for neuroprotection and tissue repair. Tissue Eng Part A 2009;15:595–604.
[35] Baumann MD, Kang CE, Stanwick JC, Wang Y, Kim H, Lapitsky Y, et al. An injectable drug delivery platform for sustained combination therapy. J Control Release 2009;138:205–13.
[36] Shoichet MS, Tator CH, Poon P, Kang C, Douglas Baumann M. Intrathecal drug delivery strategy is safe and efficacious for localized delivery to the spinal cord. Prog Brain Res 2007;161:385–92.
[37] Balazs EA. Medical applications of hyaluronan and its derivatives. J Polym Mater Sci Eng 1990;63:689–91.
[38] Balazs EA, Bland PA, Denlinger JL, Goldman AI, Larsen NE, Leshchiner EA, et al. Matrix engineering. Blood Coagul Fibrinolysis 1991;2:173–8.
[39] Vercruysse KP, Prestwich GD, Kuo JW. Hyaluronate derivatives in drug delivery. Crit Rev Ther Drug Carrier Syst 1998;15:513–55.
[40] Hollyfield JG. Hyaluronan and the functional organization of the interphotoreceptor matrix. Invest Ophthalmol Vis Sci 1999;40:2767–9.
[41] Hollyfield JG, Rayborn ME, Tammi M, Tammi R. Hyaluronan in the interphotoreceptor matrix of the eye: species differences in content, distribution, ligand binding and degradation. Exp Eye Res 1998;66:241–8.
[42] Coles BLK, Horsford DJ, McInnes RR, Van Der Kooy D. Loss of retinal progenitor cells leads to an increase in the retinal stem cell population in vivo. Eur J Neurosci 2006;23:75–82.
[43] Xu H, Iglesia DD, Kielczewski JL, Valenta DF, Pease ME, Zack DJ, et al. Characteristics of progenitor cells derived from adult ciliary body in mouse, rat, and human eyes. Invest Ophthalmol Vis Sci 2007;48:1674–82.
[44] Mori H, Fujitani T, Kanemura Y, Kino-oka M, Taya M. Observational examination of aggregation and migration during early phase of neurosphere culture of mouse neural stem cells. J Biosci Bioeng 2007;104:231–4.
[45] Hogg RE, Chakravarthy U. Visual function and dysfunction in early and late age-related maculopathy. Prog Retin Eye Res 2006;25:249–76.
[46] Tucker BA, Redenti S, Jiang C, Swift J, Klassen H, Smith M, et al. The use of progenitor cell/biodegradable MMP2-PLGA polymer constructs to enhance cellular integration and retinal repopulation. Biomaterials 2010;31:9–19.
[47] Schwartz DM, Shuster S, Jumper MD, Chang A, Stern R. Human vitreous hyaluronidase: isolation and characterization. Curr Eye Res 1996;15:1156–62.
[48] Hayasaka S, Shiono T, Hara S, Mizuno K. Lysosomal hyaluronidase in the subretinal fluid of patients with rhegmatogenous retinal detachments. Am J Ophthalmol 1982;94:58–63.
[49] Arden GB, Sidman RL, Arap W, Schlingemann RO. Spare the rod and spoil the eye. Br J Ophthalmol 2005;89:764–9.
[50] Elizabeth Rakoczy P, Yu MJT, Nusinowitz S, Chang B, Heckenlively JR. Mouse models of age-related macular degeneration. Exp Eye Res 2006;82:741–52.
[51] Ding X, Patel M, Chan CC. Molecular pathology of age-related macular degeneration. Prog Retin Eye Res 2009;28:1–18.